HHS Public Access

Author manuscript

Biomaterials. Author manuscript; available in PMC 2017 February 01.

Published in final edited form as:

Biomaterials. 2016 February ; 80: 96–105. doi:10.1016/j.biomaterials.2015.11.062.

Salmon-derived thrombin inhibits development of chronic pain through an endothelial barrier protective mechanism dependent on APC

Jenell R Smith[a], **Peter A Galie**[a,b], **David R Slochower**[a,b], **Christine L. Weisshaar**[a], **Paul A Janmey**[a,b], and **Beth A Winkelstein**[a,c,*]

[a]Department of Bioengineering, University of Pennsylvania, Philadelphia, Pennsylvania 19104

[b]Department of Physiology, Institute for Medicine and Engineering, University of Pennsylvania, Philadelphia, Pennsylvania 19104

[c]Department of Neurosurgery, University of Pennsylvania, Philadelphia, Pennsylvania 19104

Abstract

Many neurological disorders are initiated by blood-brain barrier breakdown, which potentiates spinal neuroinflammation and neurodegeneration. Peripheral neuropathic injuries are known to disrupt the blood-spinal cord barrier (BSCB) and to potentiate inflammation. But, it is not known whether BSCB breakdown facilitates pain development. In this study, a neural compression model in the rat was used to evaluate relationships among BSCB permeability, inflammation and pain-related behaviors. BSCB permeability increases transiently only after injury that induces mechanical hyperalgesia, which correlates with serum concentrations of pro-inflammatory cytokines, IL-7, IL-12, IL-1α and TNF-α. Mammalian thrombin dually regulates vascular permeability through PAR1 and activated protein C (APC). Since thrombin protects vascular integrity through APC, directing its affinity towards protein C, while still promoting coagulation, might be an ideal treatment for BSCB-disrupting disorders. Salmon thrombin, which prevents the development of mechanical allodynia, also prevents BSCB breakdown after neural injury and actively inhibits TNF-α-induced endothelial permeability in vitro, which is not evident the case for human thrombin. Salmon thrombin's production of APC faster than human thrombin is confirmed using a fluorogenic assay and APC is shown to inhibit BSCB breakdown and pain-related behaviors similar to salmon thrombin. Together, these studies highlight the impact of BSCB on pain and establish salmon thrombin as an effective blocker of BSCB, and resulting nociception, through its preferential affinity for protein C.

[*]**Correspondence to:** Beth A. Winkelstein, PhD, Department of Bioengineering, University of Pennsylvania, 240 Skirkanich Hall, 210 S. 33rd St, Philadelphia, PA 19104-6321, United States, Phone: 1-215-573-4589, Fax: 1-215-573-2071, winkelst@seas.upenn.edu.

Keywords

pain; thrombin; blood-brain barrier; activated protein C; nerve root injury

Introduction

Blood-brain barrier (BBB) disruption is characteristic of many neurological disorders, including stroke, Parkinson's disease and ALS, and contributes to the associated neuroinflammation and neurodegeneration in those diseases (1-4). The neurovasculature of the BBB is comprised of endothelial cells that are trophically coupled to nearby neurons via glial cells, which together, make up the 'neurovascular unit' and interact closely to maintain inflammatory dysfunction in disease states (5-7). The healthy BBB endothelium is bound together by tight junctions, which inhibit the transmission of serum components and blood-borne cells into the central nervous system (CNS) (6,8). BBB disruption permits the entrance of neurotoxic factors into the CNS that impair normal neuronal function and exacerbate inflammation (3,9). Peripheral nerve injuries also increase the permeability of the BBB, or more specifically the blood-spinal cord barrier (BSCB), where the injured afferents synapse (10-12). Those injuries also induce chronic neuropathic pain, which is maintained by spinal neuroinflammation (11,13,14). However, it is unclear whether BSCB disruption itself contributes to pain and should be investigated as a potential therapeutic target for chronic pain prevention. We hypothesize that a nerve root injury that initiates chronic pain also induces BSCB breakdown at times corresponding to either the development or maintenance of pain.

Systemic inflammation contributes to spinal neuroinflammation both directly and indirectly. Pro-inflammatory factors stimulate peripheral neurons that can then become hyperexcitable at their synapses in the CNS (15) and indirectly contribute to inflammation within the CNS. Circulating pro-inflammatory cytokines, such as TNF-α and IL-1β, themselves can also increase vascular permeability promoting their own entrance into the CNS across a compromised BBB (11,16-19). Once in the CNS, these inflammatory molecules directly stimulate neurons and glia, maintaining pain signaling (20,21). Further supporting the role of pro-inflammatory molecules and the development of pain, blocking the actions of TNF-α and IL-1β centrally significantly attenuates that pain that can develop after compressive nerve root injury (22). Systemic and central inflammation play important roles in pain and are integrated through BBB permeability (7,8,11); yet, it is not known whether there is a relationship between nerve root-induced pain and levels of pro- or anti-inflammatory cytokines or chemokines at times of BSCB breakdown.

The protease thrombin, most notably recognized for its role in the coagulation cascade, also regulates a variety of endothelial processes via its enzymatic activation of cell-bound receptors (23). Thrombin initiates distinct signaling cascades depending on the cofactor it binds and the substrate it cleaves (23,24,25,26). In its unbound state, mammalian thrombin increases vascular permeability by directly activating the protease-activated receptor-1 (PAR1) on the endothelial surface (23,27). In contrast, when bound to endothelial thrombomodulin, thrombin activates endothelial-bound protein C into activated protein C

(APC), which stabilizes vascular integrity (25,28,29). Clinical trials have tested APC for its enhancement of endothelial barriers in sepsis, stroke and traumatic brain injury (30-32), but its strong anticoagulant effects hamper its clinical safety (30). For this reason, a major effort in thrombin mutagenesis and protein engineering has identified domains in thrombin's structure that control protein C activation in order to increase thrombin's innate affinity for protein C instead of PAR1 by manipulating protein structure (32-35). We hypothesize that by activating the APC pathway, with either APC or thrombin with a higher affinity for protein C, will fortify the BBB and prevent pain.

Interestingly, fish differ significantly from mammals in their inflammatory responses and have naturally evolved enzymes with distinct capabilities from mammalian counterparts (36). Specifically, thrombin derived from salmon exhibits nearly indistinguishable clotting capabilities, but initiates different cell signaling cascades compared to human thrombin (36-39). Salmon thrombin induces lower levels of platelet aggregation and astrocytic transcription of pro-inflammatory cytokines compared to human thrombin at the same concentration (37,38). We have shown that salmon thrombin uniquely inhibits the development of neuropathic pain after a nerve root compression injury and activates PAR1 to a lower degree than human thrombin (38,39). We hypothesize that salmon thrombin may prevent neural pain by exhibiting a higher affinity for protein C than mammalian thrombin promoting its ability to provide vascular protection.

In this study we use a nerve root compression model in the rat to define BSCB breakdown after painful and non-painful nerve root injuries and to determine whether the resulting pain intensity correlates with serum inflammatory cytokines levels. We further investigate the effects of salmon thrombin on mediating nerve root-induced BSCB breakdown, and use in vitro studies to define its effects on inflammation-induced endothelial permeability and protein C activation. In order to establish whether directly blocking BSCB inhibits the development of pain similar to salmon thrombin, we administer intravenous APC in studies with painful nerve root injury. These three complementary studies integrate in vivo and in vitro assays and are augmented by an in silico study using protein modeling of fish and human thrombin to identify mechanistic differences that may explain the experimental observations.

Materials & Methods

Study Design & Objectives

Three experimental studies were performed to characterize BSCB breakdown, to investigate the potential for thrombin to attenuate/prevent BSCB breakdown, and to compare thrombin to known APC actions. Adult male Holtzman rats were used in all in vivo studies, and all experiments were approved by the Institutional Animal Care and Use Committee. The first set of studies characterize the time course of BSCB breakdown following painful and non-painful nerve root compression in the rat and investigate potential relationships between peripheral inflammation and pain at times of BCSB breakdown. Two durations of nerve root compression were administered in the rat: 15-minutes because it has been shown to induce sustained nociception and 3-minutes to serve as a loading control in which the nerve root undergoes injury, but pain-related behaviors do not develop (40,41). BSCB permeability

was investigated by immunolabeling the spinal cord for IgG, a blood protein that is not present in the CNS under normal conditions, at day 1 and day 7. Those time points were selected since they correspond to the development and maintenance of pain in this injury model (13,38-41). To investigate indicators of inflammation to pain and BSCB breakdown, serum levels of a panel of inflammatory cytokines were assayed at day 1, which corresponds to maximal BSCB breakdown. Of the cytokines correlating to mechanical hyperalgesia, TNF-α was the most robust and so was also immunolabeled in the spinal cord to assess whether this inflammatory mediator enters the CNS to exacerbate neuroinflammation.

The second study with salmon thrombin evaluated the effectiveness of salmon thrombin in preventing BSCB breakdown and nociception after neural injury and determines whether it acts through protein C to protect endothelial barriers. This study integrated in vivo and in vitro methods. For the in vivo portion of this study, rats undergoing painful nerve root compression were treated with salmon thrombin, human thrombin for comparison, or neurobasal media as a vehicle control. Since findings from the characterization study identified day 1 as the time point of maximal BSCB breakdown, spinal IgG was labeled and quantified on day 1 after injury with the different treatments. To test whether salmon thrombin directly protects endothelial barriers, an in vitro microchannel setup was used to measure the relative effects of salmon and human thrombin on inflammation-induced vascular permeability. Those experiments were performed in the presence of serum to expose the endothelial surface to protein C, as well as under serum-free conditions in order to examine if thrombin acts through surface receptors or serum components to modulate permeability. The production rate of APC also was compared between salmon and human thrombin using a fluorogenic peptide assay to determine if the two species exhibit different protein C activation rates.

Lastly, APC was administered after painful nerve root compression in vivo to identify whether that protein can prevent BSCB breakdown and the development of pain-related behaviors similar to salmon thrombin. In that study spinal IgG and mechanical hyperalgesia were measured on day 1 after injury. Moreover, based on the findings of these three experimental studies, we also performed protein modeling to compare the protein structures between fish and human thrombin in order to better understand how their structures influence their mechanisms of action.

Characterization of BSCB Breakdown

The right C7 nerve root was surgically exposed and compressed for 15 minutes (15min, n=10) or 3 minutes (3min, n=12) with a 10-gram force microvascular clip as previously described (41). Sham surgery (sham, n=9) included the same surgical procedures without any nerve root compression. In separate groups of rats, behavioral sensitivity was measured and spinal cord tissue was harvested on either day 1 (15min, n=5; 3min, n=7; sham n=5) or day 7 (15min, n=5; 3min, n=5; sham n=4) after injury to define the temporal pain and BSCB responses. A tester blinded to the procedure and group designation measured mechanical hyperalgesia in the ipsilateral and contralateral forepaws as a measure of radicular pain on days 1, 3, 5 and 7 as well as baseline (day 0) for a subset of the rats (42). For those rats with tissue harvested on day 1 behavioral testing occurred on days 0 and 1. Hyperalgesia was

quantified as the forepaw withdrawal threshold to an applied mechanical stimulus. The threshold was recorded as the lowest filament strength out of a series of increasing von Frey filaments that elicited a withdrawal of the forepaw upon stimulation. Thresholds for each rat on each day were determined as the average of three rounds. Paw withdrawal thresholds from the rats that were harvested on day 1 were averaged for each group on each day and were compared using two-way repeated measures ANOVA (group × day) with post-hoc Tukey's Honestly Significant Difference (HSD) Test.

Blood was collected (0.5ml) from the tail vein before surgery (baseline) and on day 1 after surgery from a subset of rats undergoing either 15 minute (n=6), 3 minute (n=4) or 0 minute (sham, n=3) nerve root compression. Serum analytes were separated and assayed for a panel of 23 pro- and anti-inflammatory cytokines and chemokines using a multiplex bead-based Luminex assay kit (#L80-01V11S5; Bio-Rad). Concentrations on day 1 were normalized to baseline levels and correlated to the normalized paw withdrawal threshold at day 1 for each rat. Each set of bivariate data (normalized threshold versus normalized cytokine concentration) was fit with a linear regression and those cytokines that strongly ($R^2>0.5$) and significantly ($p<0.05$) correlated to paw withdrawal threshold were noted.

Bilateral C7 spinal cord tissue was harvested on day 1 or day 7 in separate groups after injury in order to characterize the temporal responses of BSCB permeability. Rats were deeply anesthetized with sodium pentobarbital (65mg/kg) on the specified day and transcardially perfused with phosphate buffered saline and then 4% paraformaldehyde. Bilateral C7 spinal cord tissue was dissected, post-fixed and cryosectioned at 14μm sections. Fixed C7 spinal cord sections were fluorescently immunolabeled for rat IgG AlexaFluor 568 (1:200; Life Technologies). Images of the bilateral dorsal horns (n=3-6 sections/rat) were analyzed using a customized densitometry MATLAB code to quantify IgG labeling, which was then compared to labeling in tissue from naïve rats (39,40,43). Normalized percent IgG was compared between groups on days 1 and 7 using a two-way ANOVA (group × day) with Tukey's HSD test.

From the serum analyses, several serum cytokines were found to correlate to pain at day 1. TNF-α expression was also assayed in the spinal cord since it has previously been shown to have a role in pain and BSCB breakdown (16-19). Spinal TNF-α (1:200; Cell Signaling) was co-labeled with rat IgG in C7 ipsilateral spinal cord sections using a sequential labeling protocol with AlexaFluor 488. Visual inspection of the co-localization of spinal TNF-α and IgG was used to confirm the presence of this cytokine in areas of BSCB breakdown.

Investigation of Salmon Thrombin as a Vascular Protecting Agent

Salmon Thrombin Treatment in Vivo—Salmon thrombin (0.04U/rat; Sea Run Holdings) or human thrombin (0.04U/rat; Sigma Aldrich) was dissolved in 20μl of neurobasal media (NB media) and separately administered immediately after a 15-minute nerve root compression. Salmon thrombin (15min+STh, n=5) or human (15min+HTh, n=4) thrombin solutions were delivered directly on top of the C7 nerve root immediately after removal of the compression (38,39,43). A control group received 20μl of NB media alone to account for the effects of the vehicle (vehicle, n=5). Rats receiving sham operations (n=3), as described above, also were included as surgical controls. Rats underwent behavioral

testing prior to surgery (day 0) and on day 1 after injury and treatment. Mechanical allodynia was used to quantify behavioral sensitivity in the forepaw ipsilateral to the injury and was measured by counting the number of ipsilateral forepaw withdrawals in response to 30 stimulations by a 4g filament (38,41). The number of withdrawals was averaged for each group on each day; differences were compared using a two-way repeated measures ANOVA (group × day) with Tukey's HSD test.

At day 1, spinal cord tissue on the side ipsilateral to the injury at the C7 level was harvested and fixed for immunolabeling of spinal IgG, as described above. Differences in ipsilateral spinal IgG between groups were determined using a two-way ANOVA (group × side) with Tukey's HSD test.

Human Vein Endothelial Cell Culture & Microchannel Experiments—Human Umbilical Vein Endothelial Cell (HUVEC)-lined microchannels were created as previously reported (44). A stainless steel acupuncture needle was used to create 400μm diameter channel within a central chamber filled with collagen (2mg/ml). HUVECs were injected into the channel (10,000 cells/cm^2) and tight junctions were allowed to form by applying 24 hours of flow. After sealing the vessels, FITC-labeled dextran (70kDa) and TNF-α (100ng/ml) were perfused through the HUVEC-lined channels. Cell-lined channels were treated with dextran and TNF-α and separately stimulated with either salmon thrombin (1U/ml) or human thrombin (1U/ml). Tests were performed also with the HUVECs exposed to serum-free flow for 4 hours before stimulation by TNF-α with or without either species of thrombin. Fluorescent dextran permeation into the collagen was tracked over 10 minutes and the diameter of the flow-front was measured over time and normalized to the channel diameter (44). The slope of the normalized front diameter over time was normalized to the slope induced by TNF-α alone in order to directly compare the effects of the two species of thrombin on the flux. Experiments were run in triplicate and differences in normalized dextran flux were compared between groups using a one-way ANOVA.

Activated Protein C Substrate Assay—Salmon and human thrombin (1U/ml) were separately added to solutions containing protein C (19μg/ml; Haematologic Technologies Inc.) and a fluorogenic peptide mapping the cleavage site of the substrate for APC (Leu-Ser-Thr-Arg; 50μg/ml; Sigma Aldrich) (45). Fluorescent intensity of the solutions was read at 380nm/460nm (ex/em) every 10-seconds for 300 seconds. Controls included salmon and human thrombin separately in solution with the APC substrate in order to account for any substrate activation by the thrombins alone. Experiments were run in triplicate and differences in APC production rate induced by salmon and human thrombin were measured using a t-test.

Measuring Mechanical Hyperalgesia & Vascular Permeability after APC with Root Compression

Human activated protein C (APC) was administered intravenously (0.2mg/kg; Haematologic Technologies Inc.) as a bolus injection (5ml/kg) in sterile saline given at 1 hour after the painful 15-minute nerve root compression (15min+APC, n=5). This dosing paradigm was previously optimized to reduce vascular permeability in rat models of sepsis (46,47).

Mechanical hyperalgesia was used to quantify behavioral sensitivity in the ipsilateral forepaw before surgery (day 0) and on day 1 after surgery using the same methods as described above. The paw withdrawal threshold for the 15min+APC group was compared to injury 15min (n=5) and sham (n=5) groups from the characterization study described above using a two-way repeated measures ANOVA (group × day) with Tukey's HSD test.

As above, fixed C7 spinal cord tissue was harvested at day 1 and immunolabeled for IgG in the bilateral dorsal horns of the spinal cord to assess whether the dosing of APC was sufficient to block BSCB breakdown. The percent positive labeling of spinal IgG was compared between the 15min+APC and 15min groups and bilaterally using a two-way ANOVA (group × side) with Tukey's HSD test.

Comparative Protein Modeling of Fish and Human Thrombin

In a complementary study, the protein structures of fish and human thrombin were compared to determine if the specific regions within the thrombin structure that control substrate affinity differ between the two species of thrombin. We modeled the human thrombin autolysis loop (UniProt: P00734) into a previously validated crystal structure for human thrombin bound to a short peptide of protein C (PDB: 4DT7 chain B). The thrombin model containing the autolysis loop was created by generating 100 potential human thrombin models, and the final structure was the average of the ten models with the lowest overall Discrete Optimized Protein Energy score (48-51). The sequence for trout thrombin (UniProt: Q5NKF9) (Fig. 4), which is the most similar fully sequenced protein to salmon thrombin (25), was then threaded into the human thrombin crystal structure with an RMSD of 0.51Angstroms over 256 residues.

A model for protein C was created by submitting the full peptide sequence for protein C (UniProt: P04070) to the Protein Homology/analogY Recognition Engine V2.0 (Phyre 2) webserver (52). Using PDB code 4O03 as a template, 89% of the residues were modeled at >90% confidence. The full protein C model was refined using a steepest descent minimization in the Gromacs simulation (53) software in the presence of water and ions. A short (100ps) NVT simulation was used to further equilibrate the protein structure. The full protein C was then aligned with the short protein C peptide (QEDQVDPR) in the human thrombin structure (PDB: 4DT7) with an RMSD of 3.0Angstroms over 65 atoms.

Results

Only neural injury that induces behavioral hypersensitivity produces early BSCB breakdown

A nerve root compression applied for 15 minutes induces a significant drop ($p<0.001$) in withdrawal threshold in the forepaw ipsilateral to injury, corresponding to an increase in pain-related behaviors, on day 1, 3, 5 and 7 compared to day 0 (baseline) (Fig. 1A). The reduced threshold induced by the 15-minute nerve root compression is significantly lower ($p=0.018$) compared to sham overall and on days 1 and 7 after injury ($p<0.042$) (Fig. 1A). In contrast, a 3-minute compression does not induce a drop in threshold compared to its own

baseline threshold or sham at any day (Fig. 1A). The contralateral withdrawal thresholds are not different between any of the three groups over time (Fig. 1A).

Robust spinal IgG labeling is observed on day 1 after the painful 15-minute compression in the ipsilateral, but not contralateral, spinal cord (Fig. 1B). IgG is minimal, or not present, in the bilateral spinal cord at this time point for both of the non-painful 3-minute root compression and sham surgery (Fig. 1B). Quantification of spinal IgG and determination of differences between a 15-minute, 3-minute and 0-minute (sham) compression by two-way ANOVA (group × day; 2 degrees of freedom) reveals that a 15-minute nerve root compression induces a significant increase in IgG labeling compared to both a 3-minute compression ($p<0.001$) and sham ($p<0.001$) at day 1 after injury (Fig. 1C). The elevation in spinal IgG induced by a 15-minute compression returns to sham levels by day 7, when IgG labeling is also significantly lower ($p<0.001$) than its levels at day 1 (Fig. 1C). This early and transient increase in IgG that occurs *only* after neural injury that induces sensitivity suggests that BSCB breakdown, in regions local to neural injury, corresponds to the onset, rather than the maintenance, of pain.

At the same time when maximal BSCB breakdown is observed (day 1) after the 15-minute nerve root compression, the ipsilateral paw withdrawal threshold positively correlates to the serum concentration of four cytokines: IL-7 ($R^2=0.617$; $p=0.0015$), IL-12 ($R^2=0.572$; $p=0.0028$), IL-1α ($R^2=0.558$; $p=0.0033$) and TNF-α ($R^2=0.523$; $p=0.0052$) (Table 1; Fig. 1D). All of these are pro-inflammatory mediators and exhibit correlations with a coefficient of determination greater than 0.5. A 15-minute compression also increases TNF-α immunolabeling in the ipsilateral spinal cord at day 1 in regions that are also positively labeled for IgG (Fig. 1D). Spinal TNF-α is not evident after either the 3-minute compression or sham injury (Fig. 1D), both of which do not induce BSCB breakdown or pain at this time either (Figs. 1A-C). The co-localization of TNF-α with IgG provides evidence that increased serum concentrations of TNF-α may diffuse into the spinal cord from the blood during BSCB breakdown contributing to the development of pain-related behaviors.

Salmon thrombin inhibits BSCB breakdown through a barrier protective mechanism dependent on APC

Salmon thrombin that is applied directly to the nerve root after a 15-minute compression significantly reduces ($p=0.0148$) mechanical allodynia, quantified as the number of paw withdrawals, elicited by a 4g stimulus on day 1 compared to responses for compression treated with human thrombin. Human thrombin treatment of a 15-minute compression induces a significantly greater ($p=0.016$) number of paw withdrawals compared to sham operated rats and is not different from the responses after vehicle (neurobasal media) treatment (Fig. 2A). Paralleling the nociceptive responses, salmon thrombin induces significantly less ($p<0.0009$) IgG labeling in the ipsilateral spinal cord on day 1 compared to treatment with either human thrombin or vehicle (Fig. 2B). Both the human thrombin and vehicle treated compression injuries induce a significant increase ($p<0.0065$) in IgG in the ipsilateral spinal cord compared to the levels in the contralateral spinal cord (Fig. 2B). Together these findings suggest that salmon thrombin blocks the BSCB breakdown that

occurs after painful nerve root injury, which is a distinctly different response from that of human thrombin.

In order to investigate whether salmon thrombin actively prevents the disruption of endothelial barriers, studies were performed using collagen-housed microchannels lined with human umbilical vein endothelial cells (HUVECs) (44). TNF-α induces endothelial barrier permeability, indicated by the flux of fluorescent dextran out of the channel, in the presence and absence of serum (Fig. 2C). The addition of salmon thrombin with TNF-α to the HUVEC channels blunts the propagation of the fluorescent front into the collage, but only in the presence of serum (Fig. 2C). In contrast, human thrombin with TNF-α only exacerbates the rate of dextran flux out of the channel in the presence and absence of serum (Fig. 2C). Salmon thrombin significantly reduces ($p=0.0073$) the TNF-α-induced dextran flux through the HUVEC channels compared to human thrombin. Since salmon thrombin exhibits vascular protecting effects only when the cells are exposed to serum prior to their testing (Fig. 2C), this suggests that it may indirectly reinforce endothelial barrier stability through a component in the serum, possibly protein C (54).

To test whether salmon and human thrombin produce protein C at different rates, we measured the rate of APC substrate activation by adding salmon or human thrombin to the protein C zymogen and a fluorogenic APC substrate (45). Salmon thrombin produces APC a rate approximately 45-times faster than does human thrombin (Fig. 2D); indeed, that increased rate is significant ($p=0.008$). These data collectively suggest that salmon thrombin actively blocks inflammation-induced endothelial barrier breakdown through its unique and potent activation of the protein C.

Intravenous APC blocks BSCB breakdown and prevents pain after root injury

A painful 15-minute nerve root compression induces a significant increase ($p=0.028$) in spinal IgG in the ipsilateral compared to the contralateral side (Figs. 3A and 3B). A single intravenous injection of APC (0.2mg/kg) administered 1 hour after a 15-minute root compression significantly reduces ($p<0.0001$) ipsilateral IgG labeling at 1 day compared to the 15-minute compression alone (Figs. 3A and 3B). A 15-minute compression induces a significant drop in the paw withdrawal threshold ($p=0.024$) on day 1 compared to sham; however, treating that compression with APC prevents the drop in threshold (Fig. 3C). After treating a compression with APC the withdrawal threshold is significantly higher ($p=0.012$) than that of an untreated compression and is not different from sham (Fig. 3C). The anti-nociceptive and BSCB protective effects of APC mimic those produced by salmon thrombin (Figs. 2A-2C), lending additional supporting for the APC pathway as being beneficial at reducing BBB breakdown and pain.

Discussion

These studies show that pain induced by neural injury can be prevented by blocking early BSCB breakdown with salmon thrombin, which actively fortifies endothelial barriers under inflammatory conditions through its selective activation of protein C. The salmon thrombin treatment investigated here targets vascular dysfunction and holds promise for, not only pain prevention, but a variety of other neurological disorders for which blood-brain barrier

leakiness is a major contributor (1-4). We confirm that the development of pain-related behaviors and BSCB breakdown both occur within 1 day of a neural injury (Fig. 1). Since mechanical hyperalgesia is still present on day 7 after a painful nerve root compression when BSCB permeability returns to normal (Fig. 1), BSCB breakdown may be associated with the development, as opposed to the maintenance, of chronic nerve root-induced pain. By blocking BSCB breakdown with salmon thrombin or APC early after injury the development of hyperalgesia is completely prevented (Figs. 2 and 3), suggesting that rapid targeting of the APC pathway might eliminate the need for chronic use of analgesics later.

The treatment window for blocking BSCB is expected to be on the order of hours to a day after initial injury. We observed increased permeability of the BSCB on day 1, around the same time that pain-related behaviors develop (Fig. 1). Interestingly, both phenomena (i.e. BSCB breakdown and pain) are evident *only* after the longer compression and only ipsilaterally (Fig. 1), further supporting their association. Paralleling our findings, BSCB breakdown occurs between 6 and 24 hours after painful sciatic nerve ligation (10,11); however, ligation induces breakdown for up to 30 days in some cases (11), although we observed a return to normal by day 7 (Fig. 1). This discrepancy in duration of BSCB breakdown between our injury model and the sciatic nerve ligation models is most likely due to duration of local injury, with our compression only applied transiently and nerve ligation imposed chronically. This suggests that a more chronic nerve root compression, occurring clinically from a bulging disc or spinal stenosis, might have a larger treatment window after compression.

A limitation of the current study is that the mechanism by which peripheral neural injury induces BSCB breakdown is not investigated. The site of injury, i.e. the nerve root, is physically connected to the spinal cord through afferent axons and vasculature, suggesting that injury to one of these structures might control the breakdown. The duration of compression is important, with BSCB breakdown occurring only after the longer 15-minute and not the shorter 3-minute compression (Fig. 1). We have previously shown that electrophysiological activity in the same spinal region as that in which BSCB is observed here is maximally reduced 6.6±3.0 minutes into the root compression (40). Since this threshold of altered spinal neuronal signaling falls between the two injury durations examined in the current study, it is possible that BSCB breakdown may be neuronally controlled.

Our results further support one mechanism by which BSCB breakdown may induce pain. Serum concentrations of pro-inflammatory IL-7, IL-12, IL-1α and TNF-α correlate to mechanical hyperalgesia at day 1 (Table 1). Of these, spinal IL-1α and TNF-α have been shown to mediate nociception in this injury model (22,43). Both cytokines undergo increased transcription in the spinal cord as early as 1 hour after injury and are likely transcribed by glial cells at this time since IL-1α is exclusively localized to astrocytes in the spinal cord (43). By day 1 their transcription levels return to normal (22), but in the current study spinal TNF-α protein is still elevated at this time after painful injury (Fig. 1D). Since TNF-α expression is localized with IgG (Fig. 2B), this supports the notion that peripheral TNF-α, possibly along with other inflammatory factors, is transported from the blood into the spinal parenchyma. This spinal inflammation is evident only after the painful injury and

corresponds with increased spinal microglial and astrocytic activation that occurs by day 7 exclusively for the painful 15-minute root compression as well (41). This suggests that BSCB breakdown may facilitate the early spinal inflammation, which originates systemically, and may contribute to the sustained spinal neuroinflammation that prolongs pain (55). Further investigation of BSCB breakdown after peripheral cytokine impediment would elucidate whether these cytokines also play a significant role in barrier breakdown itself.

Although the roles of TNF-α and IL-1β in the development of pain are well-established, the contributions of IL-7 and IL-12 to pain are controversial (56-59). Clinically, IL-7 transcription and expression were shown to increase in intervertebral disc cells in patients with low back pain (59). However, serum concentrations of IL-7 in patients with cancer-related pain increase within 3 hours of an analgesic opioid treatment (57). Serum levels of IL-12 are also elevated in women with work-related musculoskeletal pain (58). In contrast, administration of IL-12 subcutaneously reduces mechanical allodynia and hyperalgesia for up to 4 hours when given after a painful chronic constriction to the sciatic nerve (56). In the current study, serum concentrations of both IL-7 and IL-12 positively correlate to mechanical hyperalgesia at day 1 after a nerve root compression (Table 1). Together with previous literature, it appears that the role of serum IL-7 and IL-12 in nociception likely depends on the source of pain. Blocking IL-7 and IL-12 systemically following painful nerve root injury would provide more information on whether elevated serum concentrations of those cytokines contribute to the development of behavioral sensitivity after nerve root compression injury.

Interestingly, IL-13, IL-10, IL-5 and IL4, which are all anti-inflammatory cytokines, also significantly correlate to mechanical hyperalgesia at day 1 after a compressive nerve root insult (Table 1); albeit none of the correlations between mechanical hyperalgesia and anti-inflammatory cytokines are as strong as those with the pro-inflammatory cytokines. Anti-inflammatory cytokines are known to stabilize vasculature; for example, administering IL-10 intrathecally for 3 days following a sciatic nerve ligation significantly reduces BSCB breakdown at day 3 (11). In the current study, the permeability of the BSCB is increased at day 1 after a painful nerve root compression when the serum expression of multiple anti-inflammatory cytokines is also elevated (Fig. 1; Table 1). Inflammation in the spinal cord and dorsal root ganglion is induced early after this neuropathic injury and is not maintained for much longer than a day (22,43). Since inflammatory cascades are a dynamic process that balance the expression levels of pro- and anti-inflammatory cytokines, the increase in anti-inflammatory cytokines at day 1 after painful nerve root compression may be a mechanism to counterbalance the early pro-inflammatory events after neural injury that produces nociception. Since spinal IgG expression is reduced by day 7 (Figs. 1B and 1C), the upregulation in anti-inflammatory cytokines might also play a role in re-establishing BSCB integrity after painful compression. Profiling the expression of these cytokines, along with BSCB breakdown, over longer time periods after nerve root compression would provide useful information about which cytokines might contribute to breakdown and which might contribute to BSCB re-stabilization.

In addition to salmon thrombin's anti-nociceptive, neuroprotective and anti-inflammatory capabilities distinct from human thrombin (38,39,60), this work is the first to show that it also uniquely blocks vessel permeability both in the spinal cord after neural injury and in HUVEC microvessels after TNF-α stimulation (Figs. 2B and 2C). Salmon thrombin prevents the early breakdown of the BSCB after neural injury, which is not evident with human thrombin or the neurobasal media vehicle (Fig. 2B). However, treatment with neurobasal media or human thrombin *does* reduce the extent of IgG extravasation into the spinal parenchyma (Figs. 1B and 2B). However, neurobasal media has been shown to marginally attenuate mechanical allodynia after this same nerve root compression and to prevent the infiltration of macrophages around the compressed root (39). In addition to the apparent anti-nociceptive and anti-inflammatory effects that are observed in vivo, it is likely that neurobasal media may also slightly attenuate compression-induced BSCB breakdown. However, since the salmon thrombin treatment prevents BSCB breakdown to a greater degree than does either the neurobasal or the human thrombin treatment (Fig. 2B), salmon thrombin's unique vascular protecting effect is likely a true finding, especially since the neurobasal media is consistently used across groups ensuring that the relative changes can be taken as useful.

Salmon thrombin's vascular stabilizing effect is also shown by its active prevention of inflammation-induced permeability in the HUVEC microchannels (Fig. 2C). Although the in vitro microchannel setup has been shown to form endothelial microvessels that are impermeable to transluminal flow (44), it does not simulate the complicated interactions between the microvascular endothelial cells, pericytes and astrocytes that make up the BSCB in vivo and therefore does not accurately model of the BBB. Despite not closely mimicking the BBB, it can serve as a suitable model for measuring the comparative effects of salmon and human thrombin on vascular permeability. We demonstrate that salmon thrombin given at 1U/ml is potent enough to combat the vascular-disrupting effects of TNF-α, whereas human thrombin is not (Fig. 2C). In biological systems, mammalian thrombin can only stabilize endothelial barriers when bound to thrombomodulin; otherwise it preferentially activates PAR1 and disrupts vasculature (27-29). The fact that salmon thrombin activates protein C even when thrombomodulin is not present (Fig. 2D) suggests that its native structure allows for it to bypass the requisite thrombomodulin binding exhibited by mammalian thrombin and directly interact with protein C. Future studies blocking APC in HUVEC microchannels prior to treatment with salmon thrombin and TNF-α would help to confirm that salmon thrombin's ability to stabilize vasculature is indeed acting through its activation of protein C.

The interaction of thrombin's exosites with various substrates guides its enzymatic specificity. In regards to protein C affinity, exosite I of human thrombin binds to the cofactor thrombomodulin, which prevents thrombin from interacting with and activating PAR1 and other substrates recognized by exosite I (61,62). There is evidence that thrombin's interaction with thrombomodulin might alter the shape of the epitope interfacing with protein C residues (63,64), facilitating that interaction. Mutagenesis studies of human thrombin have defined amino acid residues that prevent its interaction with protein C in the absence of thrombomodulin (33,35,65,66). The partial deletion of residues 146-149e, also

known as the autolysis loop (Fig. 4), increases thrombin's affinity for protein C and this sequence is highly divergent between fish and human thrombin (33). We used protein modeling to predict the relative structures of the two species of thrombin to determine if the autolysis loop might contribute to their differences in protein C affinity. The autolysis loop peptide sequence varies between the two species and is translated into a difference in predicted crystal structure (Fig. 4). Further, the crystal structures of human and fish thrombin bound to the protein C crystal suggests that the autolysis loop for both species interacts closely with protein C. The model even suggests that the autolysis loop may sterically inhibit proper binding between protein C and human thrombin more so than fish thrombin (Fig. 4). This corroborates our findings that salmon thrombin innately activates protein C with a higher efficiency than human thrombin (Fig. 2D).

In summary, the results of this study emphasize the significance of blood-brain barrier breakdown in persistent pain and support targeting early injury-induced BSCB breakdown as a novel and promising therapeutic route. Both salmon thrombin and APC ameliorate BSCB breakdown and completely inhibit the pain-related behaviors that develops after a neural injury. While APC is unsafe clinically because of its anticoagulant properties (30), salmon thrombin maintains the enzymatic ability to form fibrin clots indistinguishable from human thrombin (37,38) providing a key distinguishing feature between the two treatments. Additionally, salmon thrombin has been reported to be more stable than mammalian thrombin during gamma irradiation for sterility (67) supporting its potential safety in treating various disorders in humans.

Acknowledgments

This work was supported by the Sharpe Foundation, DOD (W81XWH-10-1-1002), NIH (T32-AR007132 and T32-HL007954) and the Ashton Foundation. We would like to acknowledge Parul Pall for her help establishing the serum collection protocol and Anna Kowalska for help with APC assays. We thank Sea Run Holdings for contributing the salmon thrombin for the in vivo and in vitro studies.

References

1. Sandoval KE, Witt KA. Blood-brain barrier tight junction permeability and ischemic stroke. Neurobiol. Dis. 2008; 32:200–219. [PubMed: 18790057]
2. Winkler EA, Sengillo JD, Sagare AP, Zhao Z, Ma Q, Zuniga E, Wang Y, Zhong Z, Sullivan JS, Griffin JH, Cleveland DW, Zlokovic BV. Blood-spinal cord barrier disruption contributes to early motor-neuron degeneration in ALS-model mice. Proc. Natl. Acad. Sci. USA. 2013; 111:E1035–E1042. [PubMed: 24591593]
3. Zlokovic BV. The blood-brain barrier in health and chronic neurodegenerative disorders. Neuron. 2008; 57:178–201. [PubMed: 18215617]
4. Zlokovic BV. Neurovascular pathways to neurodegeneration in Alzheimer's disease and other disorders. Nat. Rev. Neurosci. 2011; 12:723–738. [PubMed: 22048062]
5. Abbott NJ, Rönnbäck L, Hansson E. Astrocyte-endothelial interactions at the blood-brain barrier. Nat. Rev. Neurosci. 2006; 7:41–53. [PubMed: 16371949]
6. Abbott N NJ, Patabendige AA, Dolman DE, Yusof SR, Begley DJ. Structure and function of the blood-brain barrier. Neurobiol. Dis. 2010; 37:13–25. [PubMed: 19664713]
7. Hawkins BT, Davis TP. The blood-brain barrier/neurovascular unit in health and disease. Phramacol. Rev. 2005; 57:173–185.
8. Ballabh P P, Braun A, Nedergaard M. The blood-brain barrier: an overview: structure, regulation, and clinical implications. Neurobiol. Dis. 2004; 16:1–13. [PubMed: 15207256]

9. Webb AA, Muir GD. The blood-brain barrier and its role in inflammation. J. Vet. Intern. Med. 2000; 14:399–411. [PubMed: 10935890]
10. Beggs S, Liu XJ, Kwan C, Salter MW. Peripheral nerve injury and TRPV1-expression primary afferent C-fibers cause opening of the blood-brain barrier. Molecular Pain. 2010; 6:74. [PubMed: 21044346]
11. Echeverry S, Shi XQ, Rivest S, Zhang J. Peripheral nerve injury alters blood-spinal cord barrier functional and molecular integrity through a selective inflammatory pathway. J. Neurosci. 2011; 31:10819–10828. [PubMed: 21795534]
12. Radu BM, Bramanti P, Osculati F, Flonta ML, Radu M, Fabene PF. Neurovascular unit in chronic pain. Mediators Inflamm. 2013; 2013:648268. [PubMed: 23840097]
13. Rothman SM, Winkelstein BA. Chemical and mechanical nerve root insults induce differential behavioral sensitivity and glial activation that are enhanced in combination. Brain Res. 2007; 1181:30–43. [PubMed: 17920051]
14. Watkins LR, Milligan ED, Maier SF. Glial activation: a driving force for pathological pain. Trends Neurosci. 2001; 24:450–455. [PubMed: 11476884]
15. Szelenyi J. Cytokines and the central nervous system. Brain Res. Bull. 2001; 54:329–338. [PubMed: 11306183]
16. Hoffmann S, Grasberger H, Jung P, Bidlingmaier M, Vlotides J, Janssen OE, Landgraf R. The tumor necrosis factor-alpha induced vascular permeability is associated with a reduction of VE-caderin expression. Eur. J. Med. Res. 2002; 7:171–176. [PubMed: 12010652]
17. Huber JD, Witt KA, Hom S, Egleton RD, Mark KS, Davis TP. Inflammatory pain alters blood-brain barrier permeability and tight junctional protein expression. Am. J. Physiol. Heart Circ. Physiol. 2001; 280:H1241–H1248. [PubMed: 11179069]
18. Pan W, Kastin AJ. Tumor necrosis factor and stroke: role of the blood-brain barrier. Prog. Neurobiol. 2007; 83:363–374. [PubMed: 17913328]
19. Sharief MK, Ciardi M, Thompson EJ. Blood-brain barrier damage in patients with bacterial meningitis: associations with tumor necrosis factor-α but not interleukin-1β. J. Infect. Dis. 1992; 166:350–358. [PubMed: 1634806]
20. DeLeo JA, Yezierski RP. The role of neuroinflammation and neuroimmune activation in persistent pain. Pain. 2001; 90:1–6. [PubMed: 11166964]
21. Milligan ED, Watkins LR. Pathological and protective roles of glia in chronic pain. Nat. Rev. Neurosci. 2009; 10:23–36. [PubMed: 19096368]
22. Rothman SM, Huang Z, Lee KE, Weisshaar CL, Winkelstein BA. Cytokine mRNA expression in painful radiculopathy. J. Pain. 2009; 10:90–99. [PubMed: 18848809]
23. Di Cera E. Thrombin. Mol. Aspects Med. 2008; 29:203–354. [PubMed: 18329094]
24. Bouwens EA, Stavenuiter F, Mosnier LO. Mechanisms of anticoagulant and cytoprotective actions of the protein C pathway. J. Thromb. Haemost. 2013; 11:242–253. [PubMed: 23809128]
25. Griffin JH. Blood coagulation. The thrombin paradox. Nature. 1995; 378:337–338. [PubMed: 7477366]
26. Komarova YA, Mehta D, Malik AB. Dual regulation of endothelial junction permeability. Sci. STKE. 2007; 2007:re8. [PubMed: 18000237]
27. Coughlin SR. Thrombin signaling and protease-activated receptors. Nature. 2000; 407:258–264. [PubMed: 11001069]
28. Esmon CT. Molecular events that control the protein C anticoagulant pathway. Thromb Haemost. 1993; 70:29–35. [PubMed: 8236111]
29. Ye J, Liu LW, Esmon CT, Johnson AE. The fifth and sixth growth factor-like domains of thrombomodulin bind to the anion-binding exosite of thrombin and alter its specificity. J. Biol. Chem. 1991; 267:11023–11028. [PubMed: 1317850]
30. Bernard GR, Vincent JL, Laterre PF, LaRosa SP, Dhainaut JF, Lopez-Rodriguez A, Steingrub JS, Garber GE, Helterbrand JD, Ely EW, Fisher CJ Jr. Efficacy and safety or recombinant human activated protein C for severe sepsis. N Engl J Med. 2001; 344:699–709. [PubMed: 11236773]

31. Petraglia AL, Marky AH, Walker C, Thiyagarajan M, Zlokovic BV. Activated protein C is neuroprotective and mediates new blood vessel formation and neurogenesis after controlled cortical impact. Neurosurgery. 2010; 66:165–172. [PubMed: 20023547]
32. Zlokovic BV, Griffin JH. Cytoprotective protein C pathways and implication for stroke and neurological disorders. Trends Neurosci. 2011; 34:198–209. [PubMed: 21353711]
33. Dang QD, Sabetta M, Di Cera E. Selective loss of fibrinogen clotting in a loop-less thrombin. J. Biol. Chem. 1997; 272:19649–19651. [PubMed: 9242618]
34. Gibbs CS, Coutré SE, Tsiang M, Li WX, Jain AK, Dunn KE, Law VS, Mao CT, Matsumura SY, Mejza SY, Paborsky LR, Leung LLK. Conversion of thrombin into an anticoagulant by protein engineering. Nature. 1995; 378:413–416. [PubMed: 7477382]
35. Marino F, Pelc LA, Vogt A, Gandhi PS, Di Cera E. Engineering thrombin for selective specificity toward protein C and PAR1. J. Biol. Chem. 2010; 285:19145–19152. [PubMed: 20404340]
36. Doolittle RF. Coagulation in vertebrates with a focus on evolution and inflammation. J Innate Immun. 2011; 3:9–16. [PubMed: 20980726]
37. Michaud SE, Wang LZ, Korde N, Bucki R, Randhawa PK, Pastore JJ, Falet H, Hoffmeister K, Kuuse R, Uibo R, Herod J, Sawyer E, Janmey PA. Purification of salmon thrombin and its potential as an alternative to mammalian thrombins in fibrin sealants. Thromb. Res. 2002; 107:245–254. [PubMed: 12479886]
38. Smith JR, Syre PP, Oake SA, Nicholson KJ, Weisshaar CL, Cruz K, Bucki R, Baumann BC, Janmey PA, Winkelstein BA. Salmon and human thrombin differentially regulate radicular pain, glial-induced inflammation and spinal neuronal excitability through protease-activated receptor-1. PLoS One. 2013; 8:e80006. [PubMed: 24278231]
39. Weisshaar CL, Winer JP, Guarino BB, Janmey PA, Winkelstein BA. The potential for salmon fibrin and thrombin to mitigate pain subsequent to cervical nerve root injury. Biomaterials. 2011; 32:9738–9746. [PubMed: 21944723]
40. Nicholson KJ, Quindlen JC, Winkelstein BA. Development of a duration threshold for modulating evoked neuronal responses after nerve root compression injury. Stapp Car Crash J. 2011; 55:1–24. [PubMed: 22869302]
41. Rothman SM, Nicholson KJ, Winkelstein BA. Time-dependent mechanics and measures of glial activation and behavioral sensitivity in a rodent model of radiculopathy. J. Neurotrauma. 2010; 27:1–12. [PubMed: 19698073]
42. Chang YW, Winkelstein BA. Schwann cell proliferation and macrophage infiltration are evident at day 14 after painful cervical nerve root compression in the rat. J. Neurotrama. 2011; 28:2429–2438.
43. Rothman SM, Winkelstein BA. Cytokine antagonism reduces pain and modulates spinal astrocytic reactivity after cervical nerve root compression. Ann. Biomed. Eng. 2010; 38:2563–2576. [PubMed: 20309734]
44. Galie PA, Nguyen DH, Choi CK, Cohen DM, Janmey PA, Chen CS. Fluid shear stress threshold regulates angiogenic sprouting. Proc. Natl. Acad. Sci. USA. 2014; 111:7968–7973. [PubMed: 24843171]
45. Ohno Y, Kato H, Morita T, Iwanaga S, Takada K, Sakakibara S, Stenflo J. A new fluorogenic peptide substrate for vitamin k-dependent blood coagulation factor, bovine protein C. J. Biochem. 1981; 90:1387–1395. [PubMed: 6896048]
46. Keller SA, Moore CC, Evans SL, McKillop IH, Huynh T. Activated protein C alters inflammation and protects renal function in sepsis. J. Surg. Res. 2011; 168:e103–e109. [PubMed: 21429520]
47. Teke Z, Sacar S, Yenisey C, Atalay AO, Kavak T, Erdem E. Role of activated protein C on wound healing process in left colonic anastomoses in the presence of intra-abdominal sepsis induced by cecal ligation and puncture: an experimental study in the rat. World Surg. J. 2008; 32:2434–2443.
48. Eswar N, Webb B, Marti-Remon MA, Madhusudhan MS, Eramian D, Shen M, Pieper U, Šali A. Comparative protein structure modeling using Modeller. Curr Protoc Bioinformatics Chapter 5:Unit 5. 2006
49. Martí-Renom MA, Stuart AC, Fiser A, Sánchez R, Melo F, Šali A. Comparative analysis protein structure modeling of genes and genomes. Annu Rev Biophys Biomol Struct. 2000; 29:291–325. [PubMed: 10940251]

50. Šali A, Blundell TL. Comparative protein modeling by satisfaction of spatial restraints. J Mol Biol. 1993; 243:779–815. [PubMed: 8254673]
51. Fiser A, Do RKG, Šali A. Modeling of loops in protein structures. Protein Sci. 2000; 9:1753–1773. [PubMed: 11045621]
52. Kelley LA, Sternberg MJE. Protein prediction on the web: a case study using the Phyre server. Nat Protoc. 2009; 4:363–371. [PubMed: 19247286]
53. Pronk S, PálL S, Schulz R, Larsson P, Bjelkmar P, van der Spoel D, Hess B, Lindahl E. GROMACS 4.5: a high-throughput and highly parallel open source molecular simulation toolkit. Bioinformatics. 2013; 29:845–854. [PubMed: 23407358]
54. Riewald M, Petrovan RJ, Donner A, Mueller BM, Ruf W. Activation of endothelial cell protease activated receptor 1 by the protein C pathway. Science. 2002; 296:1880–1882. [PubMed: 12052963]
55. Bowels RD, Mata BA, Bell RD, Mwangi TK, Huebner JL, Kraus VB, Setton LA. In vivo luminescence imaging of NF-κB activity and serum cytokine levels predict pain sensitivities in a rodent model of osteoarthritis. Arthritis Rheumatol. 2014; 66:637–646. [PubMed: 24574224]
56. Chen IF, Khan J, Noma N, Hadlaq E, Teich S, Benoliel R, Eliav E. Anti-nociceptive effect of IL-14p40 in a rat model of neuropathic pain. Cytokine. 2013; 62:401–406. [PubMed: 23597590]
57. Heitzer E, Sandner-Kiesling A, Schippinger W, Stohscheer I, Osprain I, Bitsche S, Eisner F, Verebes J, Hoffmann G, Samonigg H. IL-7, MCP-1, MIP1-bets, and OPG as biomarkers for pain treatment response in patients with cancer. Pain Physician. 2012; 15:499–510. [PubMed: 23159968]
58. Matute Wilander A, Karedal M, Axmon A, Nordander C. Inflammatory biomarkers in serum in subjects with and without work related neck/shoulder complaints. BMC Musculoskelet Disord. 2014; 15:103. [PubMed: 24669872]
59. Zhang Y, Chee A, Shi P, Adams SL, Markova DZ, Anderson DG, Smith HE, Deng Y, Plastaras CT, An HS. Intervertebral disc cells produce interleukins found in patients with back pain. Am. J. Phys. Med. Rehabil. 2015
60. Uibo R, Laidmäe I, Sawyer ES, Flanagan LA, Georges PC, Winer JP, Janmey PA. Soft materials to treat central nervous system injuries: evaluation of the suitability of non-mammalian fibrin gels. Biochim. Biophys. Acta. 2009; 1793:924–930. [PubMed: 19344675]
61. Fuentes-Prior P, Iwanaga Y, Huber R, Pagila R, Rumennik G, Seto M, Morser J, Light DR, Bode W. Structural basis for the anticoagulant activity of the thrombinthrombomodulin complex. Nature. 404:518–525. [PubMed: 10761923]
62. Pineda AO, Chen ZW, Caccia S, Cantwell AM, Savvides SN, Waksman G, Mathews FS, Di Cera E. The anticoagulant thrombin mutant W215A/E217A has a collapsed primary specificity pocket. J. Biol. Chem. 2004; 279:39827–39828.
63. Xu H, Bush LA, Pineda AO, Caccia S, Di Cera E. Thrombomodulin changes the molecular surface of interaction and the rate of complex formation between thrombin and protein C. J. Biol. Chem. 2005; 280:7956–7961. [PubMed: 15582990]
64. Ye J, Esmon NL, Esmon CT, Johnson AE. The active site of thrombin is altered upon binding to thrombomodulin. Two distinct structural changes are detected by fluorescence, but only one correlates with protein C activation. J. Biol. Chem. 1991; 266:23016–23021. [PubMed: 1660464]
65. Rezaie AR, Yang L. Thrombomodulin allosterically modulates the activity of the anticoagulant thrombin. Proc. Natl. Acad. Sci. USA. 2003; 100:12051–12056. [PubMed: 14523228]
66. Yang L, Manithody C, Rezaie AR. Activation of protein C by the thrombinthrombomodulin complex: cooperative roles of Arg-35 of thrombin and Arg-67 of protein C. Proc. Natl. Acad. Sci. USA. 2006; 103:879–884. [PubMed: 16418283]
67. Laidmäe I, McCormick ME, Herod JL, Pastore JJ, Salum T, Sawyer ES, Janmey PA, Uibo R. Stability, sterility, coagulation, and immunologic studies of salmon coagulation proteins with potential use for mammalian wound healing and cell engineering. Biomaterials. 2006; 27:5771–5779. [PubMed: 16919721]

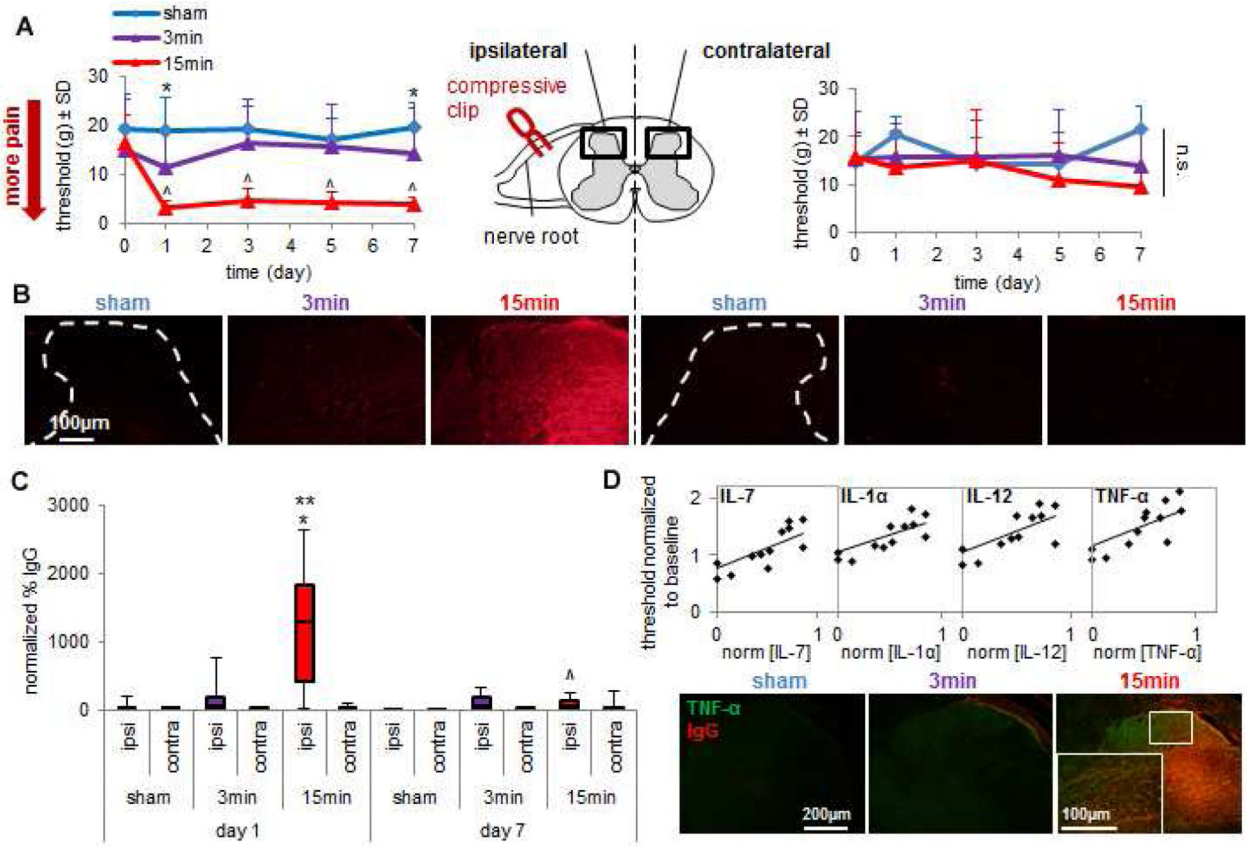

Fig. 1. Peripheral neural injury causes early BSCB breakdown and inflammation corresponding to the onset of behavioral hypersensitivity

(A) A 15-minute nerve root compression significantly decreases (^p<0.001) the withdrawal threshold in the ipsilateral forepaw on each day compared to corresponding baseline thresholds. That 15-minute compression also significantly decreases the withdrawal threshold compared to sham overall (p=0.018) and on individual days 1 and 7 (*p<0.042). Thresholds in the contralateral forepaw are not different between groups.Data are shown as mean±SD. **(B)** Representative images depict intense IgG labeling only in the ipsilateral dorsal horn on day 1 after 15min. Minimal bilateral IgG labeling is evident on day 1 for 3min and sham. **(C)** The percent IgG labeling in the ipsilateral spinal cord significantly increases at day 1 after 15min compared to sham (*p<0.001) and 3min (**p<0.001). By day 7, ipsilateral IgG significantly decreases (^p<0.001) compared to day 1. Data are mean±SD. **(D)** On day 1, withdrawal threshold positively correlates to the serum concentration of four pro-inflammatory cytokines: IL-7, IL-12, IL-1α and TNF-α (see Table 1). Ipsilateral spinal TNF-α immunoreactivity also increases in areas of BSCB breakdown on day 1 only for 15min.

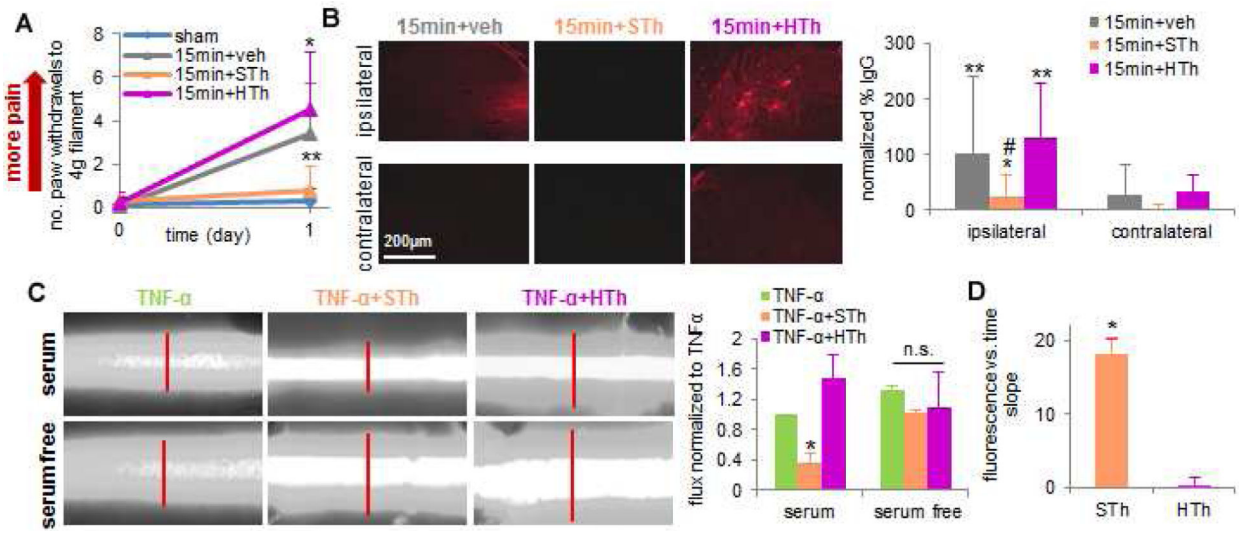

Fig. 2. Salmon thrombin prevents vascular disruption dependent on protein C

(A) Mechanical allodynia (quantified by the number of paw withdrawals) is significantly reduced (**p=0.0148) on day 1 after compression treated with salmon thrombin (15min +STh) compared to human thrombin (15min+HTh). Allodynia for 15min+HTh is significantly greater (*p=0.016) than sham and not different from vehicle-treatment with compression (15min+veh). **(B)** There is minimal IgG labeling after 15min+STh in the ipsilateral dorsal horn on day 1, and is significantly less than 15min+HTh (*p<0.0001) and 15min+veh (#p=0.0009). Both 15min+HTh and 15min+veh exhibit robust ipsilateral spinal IgG labeling that is significantly greater (**p<0.0065) than the labeling in the respective contralateral sides. **(C)** HUVEC-lined microchannels exhibit increased FITC-dextran flux into the surrounding collagen when treated with TNF-α with or without serum. Salmon thrombin (TNF-α+STh) significantly reduces (*p=0.0073) TNF-α-induced flux compared to human thrombin (TNF-α+HTh) only in the presence of serum. TNF-α+STh and TNF-α +HTh are not different in serum-free conditions. **(D)** STh produces APC significantly faster (*p=0.008) than HTh. All data are mean±SD.

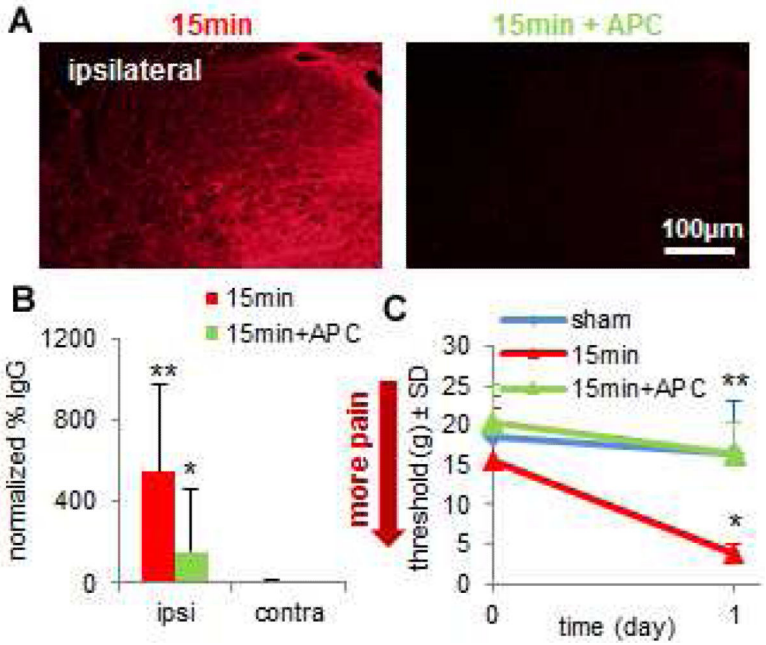

Fig. 3. Blocking BSCB breakdown with intravenous APC inhibits nociception after neural injury

(A) Spinal IgG is reduced after APC treated 15-minute compression (15min+APC) compared to compression alone (15min). **(B)** A 15min compression significantly increases (**p=0.028) spinal IgG in the ipsilateral dorsal horn compared to the contralateral dorsal horn on day 1. Ipsilateral IgG for 15min+APC is significantly lower (*p<0.001) than 15min on day 1 and is not different from respective contralateral values. **(C)** Forepaw withdrawal threshold at day 1 is significantly reduced (*p=0.024) by a 15min compression compared to sham, whereas, 15min+APC exhibits a significantly higher (**p=0.012) withdrawal threshold than 15min, which is not different sham. All data represented as mean±SD.

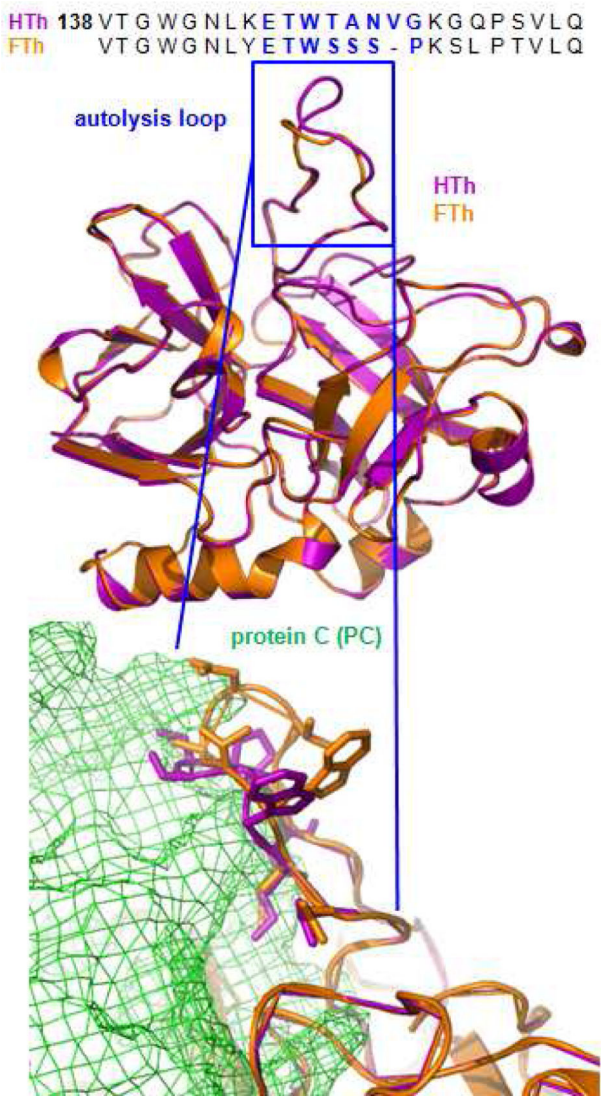

Fig. 4. Protein structure for thrombin derived from fish and from human differs in the autolysis loop, which partially controls thrombin's specificity for protein C

Aligned amino acid sequences for the B chains of human thrombin (HTh) and fish thrombin (*Salmo gairdneri*, FTh) exhibit a key divergence in the autolysis loop (blue). A crystal structure for HTh (magenta) bound to a small peptide of protein C (PDB:4DT7) and the created homology model for FTh (orange) have strong alignment (RMSD=0.51Å over 265 residues) shown in ribbon representation. The autolysis loop (in blue) does not retain the same structure between species. The residues within both autolysis loops are represented below as sticks to visualize predicted close interactions with protein C (green cage structure).

Table 1

Serum levels of 23 pro- and anti-inflammatory cytokines and chemokines (x) and their correlation to ipsilateral forepaw withdrawal threshold (y) on day 1 after neural injury.

cytokine	correlation	R^2	p-value
pro-inflammatory			
IL-7	y=0.74x+0.77	**0.617**	**0.0015**
IL-12	y=0.73x+1.78	**0.572**	**0.0028**
IL-1α	y=0.57x+1.07	**0.558**	**0.0033**
TNF-α	y=0.72x+1.18	**0.523**	**0.0052**
VEGF	y=0.43x+1.04	0.485	**0.0082**
IL-17	y=0.43x+0.98	0.479	**0.0087**
G-CSF	y=0.66x+1.14	0.456	**0.0113**
IL-1β	y=0.72x+1.04	0.446	**0.0126**
MIP-3α	y=0.37x+1.03	0.422	**0.0162**
IFN-γ	y=0.56x+1.09	0.376	**0.0258**
IL-2	y=0.41x+1.02	0.345	**0.0348**
IL-18	y=0.58x+1.01	0.283	0.0613
GM-CSF	y=0.89x+1.25	0.173	0.1574
GRO/KC	y=0.71x+1.13	0.163	0.1707
RANTES	y=0.12x+0.98	0.042	0.5031
anti-inflammatory			
IL-13	y=0.68x+1.04	0.496	**0.0072**
IL-10	y=0.42x+0.94	0.439	**0.0137**
IL-5	y=0.27x+0.99	0.415	**0.0175**
IL-4	y=0.50x+1.02	0.383	**0.0241**
EPO	y=0.56x+1.00	0.344	**0.0352**
MCP-1	y=0.21x+1.01	0.182	0.1459
both pro- and anti-inflammatory			
IL-6	y=0.56x+1.09	0.356	**0.0315**
M-CSF	y=0.21x+1.01	0.321	**0.0434**

Note: shaded cells indicate R^2 greater than 0.5.